3D THERMAL AND CFD SIMULATIONS OF THE DIVERTOR MAGNETIC COILS FOR ITER

Anna Encheva [(1) a], **George Vayakis** [b], **Rene Chavan** [a], **Alexander Karpouchov** [a], **Jean-Marc Moret** [a]

[a] **Ecole Polytechnique Fédérale de Lausanne (EPFL)**
Centre de Recherches en Physique des Plasmas
Association Euratom-Confédération Suisse
CH-1015 Lausanne, Switzerland

[b] **ITER International Team, Boltzmannstr.2, 85748 Garching, Germany**

SUMMARY

Magnetic diagnostics for the new generation fusion reactor “ITER” are required to be extremely reliable since they provide measurements essential for reactor operation and protection, plasma control and for measurement of several parameters fundamental to the plasma operation, such as plasma current and shape, disruptions and high frequency macro instabilities.

ITER magnetic diagnostics consist of various sets of inductive coils and loops mounted on the inner wall, outside the vacuum vessel and in some of the divertor cassettes [[1]]. All these probes measure magnetic field or flux variations with respect to time, requiring a precise integration of the signals to recover the absolute values of the field components. They operate in a harsh reactor environment, subjected to nuclear heat loads mainly due to the neutron radiation, generated by the burning plasma. Difficult or impossible access after assembly requires reliability, especially in the area of wiring, connections and vacuum feed-throughs and in choosing margin against radiation damage and extreme transient electrical loads. Additional disturbing effects can arise when both a strong transient magnetic field and thermal gradient occur within the coil structure. All these aspects set a serial of strict design requirements and imply a serious technical challenge.

This paper is focused on the design, simulation and optimization of the ITER divertor magnetic tangential coils. The divertor is one of the components

[1] Corresponding author Tel.: +41 21 6931939; fax: +41 21 6935176.

E-mail address: anna.encheva@epfl.ch (A.Encheva, Dr.Dipl.Eng, Mechanical Engineer - Scientist)

exposed to the highest heat load in a fusion reactor, with a surface thermal peak load of 20 MW/m^2. About 15 % of the energy produced by fusion reactions is absorbed in the divertor region. The radially-oriented divertor cassettes are exposed to inhomogeneous and time-dependent neutron flux. Six similar divertor cassettes are instrumented for magnetic measurements. Six pairs of equilibrium coils (normal and tangential to the mounting surface) are mounted within each of these cassettes. Of those, pairs near the top region of divertor dome will be exposed to the highest nuclear heating of all magnetic sensors, 2.5 MW/m^3.

The most critical issue for the divertor coils is to minimise Radiation Induced Thermo-Electric Sensitivity (RITES) [2] and Thermally Induced Electromagnetic Force (TIEMF) [3] by combining a proper choice of conductor with low temperature variation in the coil. Instead of Mineral Insulated Cable (MIC), which was foreseen as the preferred winding for the magnetic coils, a winding made of ceramic-coated steel wire was recently proposed [4]. It is thought that, for this wire, maintaining a temperature variation in the wiring below 10K will be sufficient to allow long-pulse operation. Variations of the divertor coil design have been investigated and simulated with the help of ANSYS programme. The aim was to keep the temperature variation in the winding pack within this limit. The optimisation of the coil, based only on a cooling by conduction was not sufficient to meet the 10 K target. Therefore, an actively water cooled coil was designed and simulated by the CFD code – ANSYS CFX.

1: Introduction

The divertor is one of the components being exposed to the highest peak heat loads in the fusion reactor. About 15 % of the energy produced by fusion reactions must be removed through the divertor, yielding a thermal peak heat flux of up to 20 MW/m^2, which constitutes a significant technical challenge to the divertor target surfaces and makes them a difficult structure for the direct mounting of magnetic sensors. Preliminary studies, concentrated mainly on the improvement of the divertor cassettes and of the magnetic probes were started during the second half of 1993 [5]. A summary of the reference design can be found in the ITER FDR [6]. It has 56 cassettes, cooled by water provided by pipes routed through the lower pumping ports. The cassettes are removable and the plasma-facing targets can be exchanged in the ITER hot cell. At present it is assumed that sufficient intrinsic redundancy will be provided in the divertor probes to avoid having to replace the coils for the ITER lifetime (and through one or more target exchange operations). Clearly, the whole cassette body or a sensor sub-assembly can also be exchanged in the hot cell as a last resort.

More recently, the existing divertor design has been significantly changed and several modifications of the shape, materials, supports, etc. of the divertor dome/liner are still under consideration. These will mainly affect the exact sensor positions and maximum size.

Divertor equilibrium coils are an essential supplement to the in-vessel magnetics set for the measurement of separatrix-wall gaps and reconstruction of equilibria (plasma shape and position) In general, the closer is the sensor to the plasma, the better the reconstruction accuracy. On the other hand, this makes the coil design more complicated due to the necessity to protect the coils from the plasma neutron radiation. The divertor coils are found to improve the reconstruction accuracy near the X-point by about a factor of 3, bringing it close to the ITER measurement requirements.

Additional effects potentially reducing the operational reliability are thermoelectrically and radiation induced potentials in and along the signal conducting and coiled cables, which depend on the type of the cable chosen. A margin for these effects should also be considered in the coil design.

The general principles relevant to the in-vessel magnetic probes are also valid for the divertor coils [4]. The induction coil or pick-up coils, the most widely used vector measuring instruments, are based on Faraday's law. If we considerer that the winding volume could be placed in a uniform magnetic induction field parallel to the sensor axis constituted by a cylindrical coil having area **A** and **N** turns then the inducted electromotive-force is:

$$e.m.f = -NA\frac{d}{dt}B(t) = K\frac{d}{dt}B(t) \qquad \textbf{(Eq. 1)}$$

where **K** is the calibration constant of the coil.

The analogue integration of the voltage measured permits to obtain the value of the induction magnetic field. The winding constitutes a tight spiral along the axis, in order to be protected from the transversal field and to avoid parasitic distortion in the measurement. The choice of the return path of the conductor is also very important in order to improve stability towards transversal fields.

2: Description of the location and design of the coil

The main function of the divertor system is to exhaust the major part of the alpha particle power as well as impurities from the plasma. The divertor has a very complex geometry and mainly consists of two types of components: the high heat flux (HHF) components able of removing the high heat loads which are typical for this domain and at the same time providing neutron shielding for the vacuum vessel and the magnet coils in the vicinity of the divertor, and an underlying "Cassette Body" which function is to keep in place the HHF components.

The exact location of the coils is still under discussion. According to the latest distribution of the divertor coils the following locations, shown in Fig.1 [7], are considered: one pair of a tangential and a normal coil behind the inner Vertical Targets, two pairs behind the outer Vertical Targets (VT) (one in the lower part and one in the upper part, close to the Baffles), one pair under the Dome, and one pair under the inner and under the outer neutral particle reflector (plates that together with the lower ends of the VT form a "V" shape).

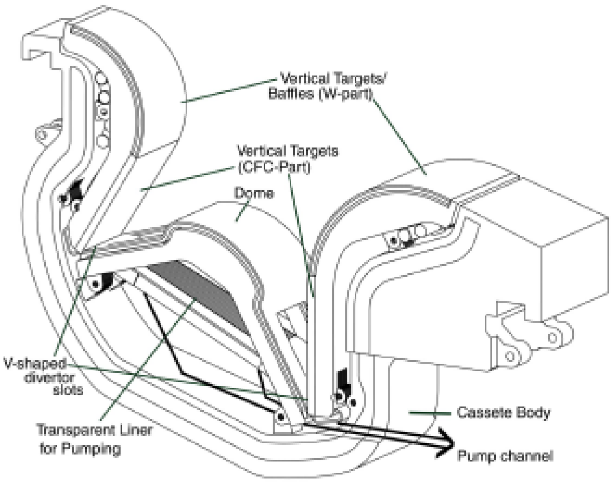

Figure 1: Divertor cassette layout

The most critical issue for the divertor coils, besides the requirement of withstanding the high heat loads due to nuclear heating, is to minimise Radiation Induced Thermo-Electric Sensitivity (RITES) and Thermally Induced Electromagnetic Force (TIEMF) [3] by combining a proper choice of conductor with low temperature variation in the coil. For these reasons, few improvements of the design described below have been calculated numerically. Instead of Mineral Insulated Cable (MIC), which was foreseen as the preferred winding for the magnetic coils, a winding made of ceramic-coated steel wire was proposed [4]. It is thought that, for this wire, maintaining a temperature variation in the wiring below 10 K will be possible and also sufficient to allow long-pulse operation. It is planned to test this assumption by specific R&D, including irradiation of complete coils in fission reactors. The design of the inner vessel pick-up coils has been considered as a base layout for the tangential divertor coils. Fig.2 shows ¼ of the coil – half along the length and half along the

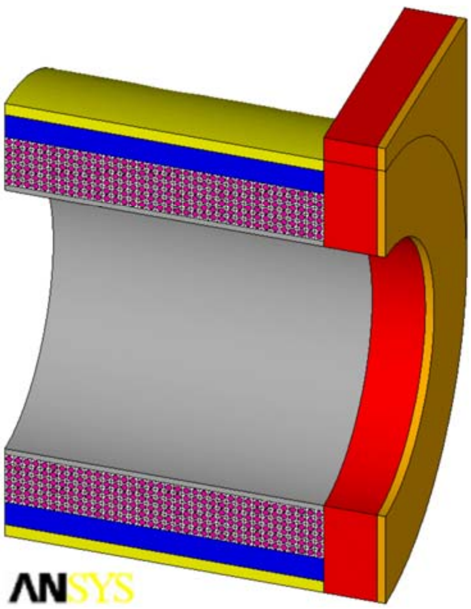

Figure 2: FEM model of ¼ of the tangential divertor coil

circumference. The coil consists of: a former (dark grey), made of stainless steel with thickness 0.5 mm, a case (yellow), made of copper 1 mm with thickness, end-plates – made of copper (red) with thickness 4.2 mm and second end-plate (orange) made of steel with 0.7 mm thickness, necessary for fixing the coil on the cassette body structure, a ceramic filler (blue) with thickness of 2mm, and a conductor which comprises of 6 layers x 36 windings (per layer) of ceramic coated steel wire. The steel wire (magenta) has a diameter of 0.5 mm in cross-section and the ceramic coating (white) has a thickness of 0.1 mm.

3: Computer Modelling

Variations of the in-vessel tangential coil design, described above, have been investigated and simulated with the help of ANSYS program [8]. The main objective was to find the optimal design in which the temperature variation in the winding pack, after applying divertor relevant nuclear heat load conditions, does not exceed 10 K. Three-dimensional, thermal, steady-state analyses have been performed. Parametric ANSYS input files for the different cases have been established which can be modified and easily run many times. Due to the symmetry of the model along the XY axis and along the circumference, only ¼ of the coil has been simulated.

The material properties used in the simulation are listed in Table 1. The variation of the properties with temperature is often critical for obtaining an accurate simulation's result. In our case, the temperature variation in the coil structure is not significant which allows us to use non-temperature dependent material properties.

	Density (kg/m^3)	Thermal Conductivity (W/m.K)	Specific heat (J/kg.K)
Stainless steel	8060	16.3	500
Copper	8920	385	450 [9]
Ceramic	3900	1.71	385

Table 1: Temperature invariant material properties used in the simulation

The 3D thermal conduction element SOLID70 which has eight nodes with a single degree of freedom - temperature at each node, is used to simulate the behaviour of the coil. One single comparison between SOLID70 and SOLID90 has been performed. Even though, using SOLID90 can lead to a more precise prediction because it has 20 nodes with a degree of freedom - temperature on the mid-nodes as well, by comparing the results it could be concluded that the difference in the temperature distribution is not significant and for this reason a good compromise between computing time and accuracy of the results is the element type SOLID70. In order to obtain a uniform and accurate mesh a 2D mesh is first generated in the cross-section of the coil, along the XY axis, and then cylindrical volumes are generated by rotating the area patterns. The total number of elements in this case is approximately 232 000.

4: Boundary conditions and loads

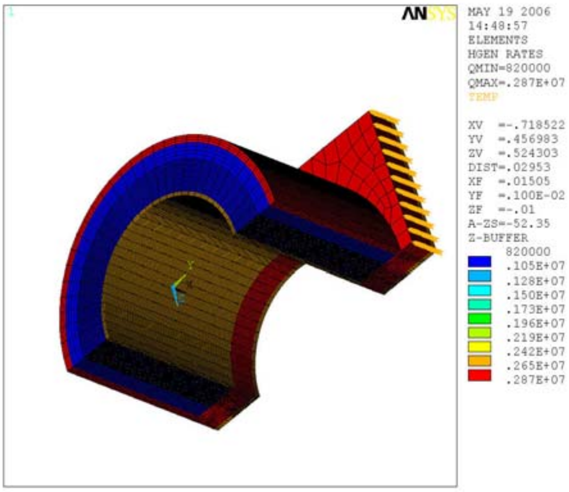

Figure 3: Heat generation rate and temperature applied on the coil

For the simulation the coil located under the dome (see Fig.1) is taken into consideration, since it is the only one subjected to the highest nuclear heating rate. Volumetric heat generation resulting from the nuclear heating relevant to the divertor region was imposed on the different material of the coil: for stainless steel 2.5 $x10^6$ W/m^3, for copper 2.875 $x10^6$ W/m^3, for ceramic 0.82 $x10^6$ W/m^3. A temperature of 393.15 K is applied on the nodes of the end-plates, as shown on Fig.3, which corresponds to the assumed surface temperature of the cassette body components on which the coils should be mounted.

5: Results

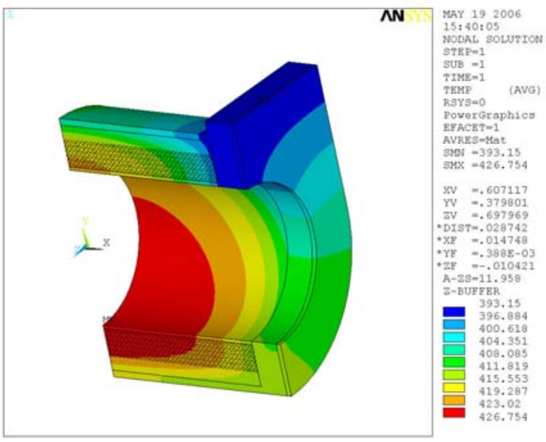

Figure 4: Temperature distribution (Kelvin) by using SOLID70

From Fig.4, Fig.5 and Fig.6 could be seen that using SOLID90 element type leads to slightly higher temperature in the coil structure. The reason for this more exact prediction is that a heat generation is applied not only on the corner nodes of each single element, but on each midside node as well, and the value is equal to the average heat generation rate of its adjacent corner nodes. The temperature increase along the azimuthal direction within one winding (path 1, see Fig.5 and Fig.6) show that the temperature difference in the wire-longitudinal direction is 7.27 K. On the contrary, the temperature difference along the X-axis (path 2, see Fig.5, Fig.6) is approximately 23.5K. The ripple on the curve in Fig.5 is due to the fact that some nodes of path 1 are attached to the steel wire and some are part of the ceramic coating - two materials having different thermal conductivity values.

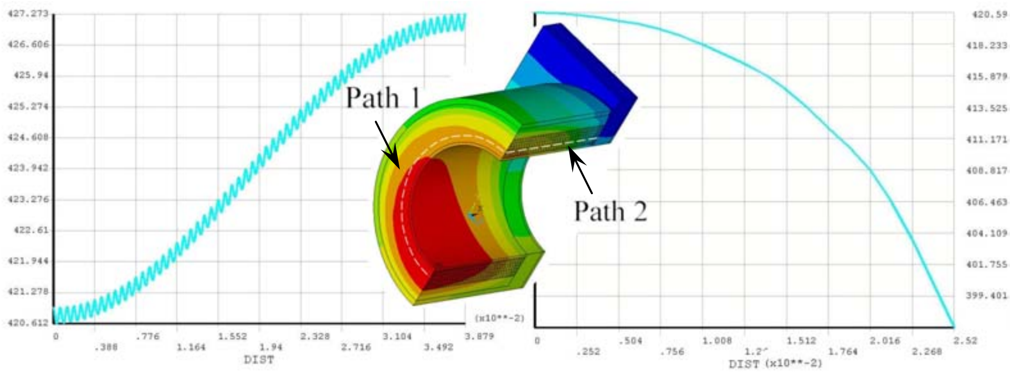

Figure 5: Temperature increase (Kelvin) along azimuthal direction with SOLID90

Figure 6: Temperature decrease (Kelvin) along X-axis

<u>5.1. First design optimisation</u>

The first optimisation presents a reshaping of the coil. Instead of 6 layers with 36 windings each, there are 9 layers with 24 windings per layer. The total number of turns remains unchanged – 432. The overall dimensions of the coil, the choice of materials, and boundary conditions and loads are as already described in the previous topics. The temperature distribution is shown in Fig.7 and Fig.8 in different view perspectives.

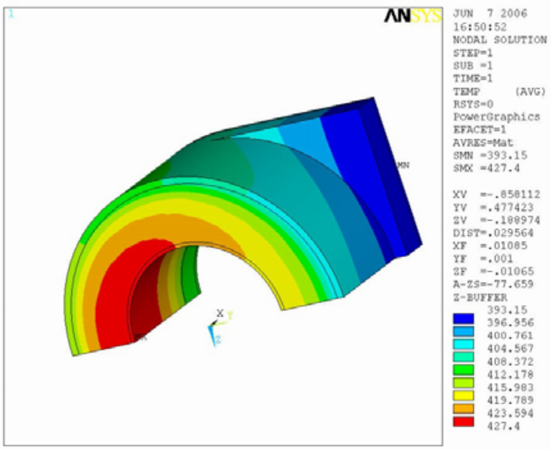

Figure 7: Temperature distribution (Kelvin), reshaped model, backside

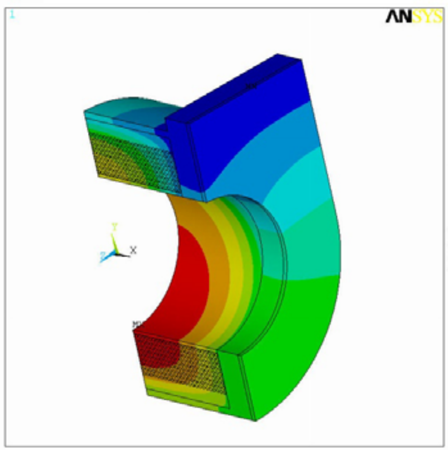

Figure 8: Temperature distribution (Kelvin), reshaped model, sideview

Reshaping of the coils does not contribute much to the overall decrease of the temperature in the coil structure. The temperature difference along the azimuthal direction is 9 K and along the X-axis is 19K.

5.2. Second design optimisation

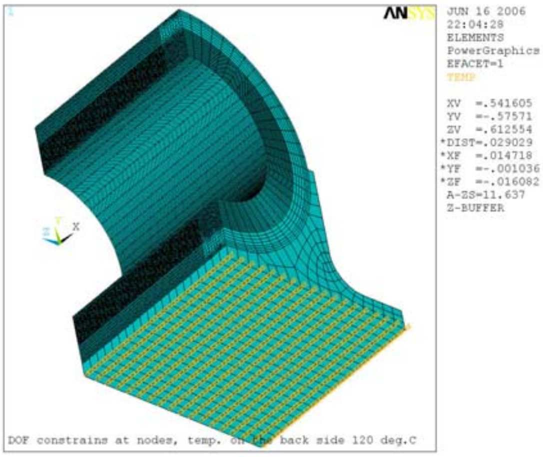

Figure 9: Temperature DOF applied on the backside

In the second optimisation the coil itself remains unchanged. The end plates maintain the same shape as the coil and consist of 2mm thick copper plate and 2mm thick steel plate. An additional jacket is modelled for fixing the coil on the newly proposed mounting structure placed in each divertor cassette.

A temperature degree of freedom is applied on each node at the back side of the jacket, as it is shown in Fig.9. Two different cases have been simulated, in the first model the jacket is made of stainless steel and in the second model it is made of copper. The overall dimensions, the choice of material and the applied heat generation rates in the coil structure remain exactly the same, as described in section 4. The temperature distribution for both cases is shown in Fig.10 and Fig.11, respectively.

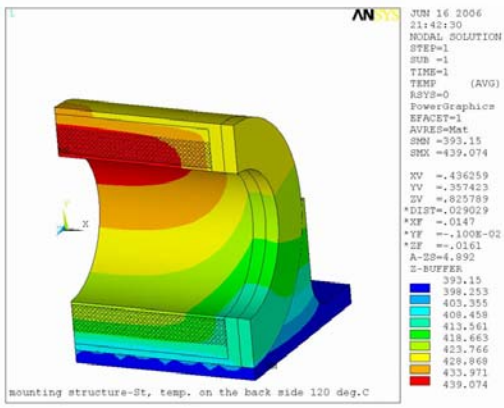

Figure 10: Temperature distribution (Kelvin), steel jacket

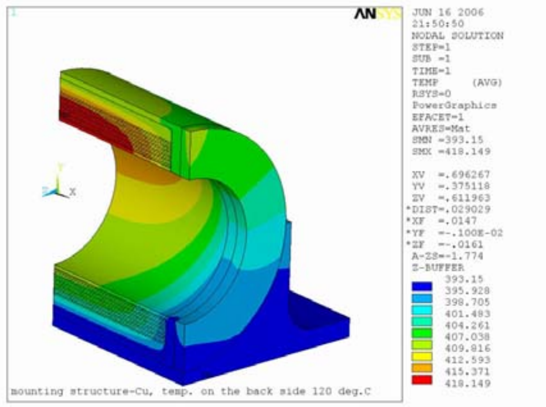

Figure 11: Temperature distribution (Kelvin), copper jacket

According to the simulation done the best result achieved seems to be a coil with jacket made of copper. It is observed that the jacket serves as well for extending the heat conduction path from the inner part of the coil to the endings which leads to the reduced temperature. The temperature variation in the coil in this case is 25°C, compared to $\Delta T = 44.9$°C in the case of jacket made of steel, $\Delta T = 34.2$°C in the reshaped coil – 9 layers x 24 windings, and $\Delta T = 33.6$°C in the original design having 6 layers x 36 windings and 4.2mm copper end-plate and 0.7mm steel end-plate.

Though there is a visible improvement in the thermal behaviour of the coil due to the proposed design optimisations, the results are still far beyond the set target of 10 K. It could be concluded that a design based only on a cooling by conduction is not sufficient to withstand the high heat loads and to keep the temperature in the coil within the required limits. Therefore, after matching the constraints for coil performance (effective area, size and frequency response) to the space constraints in the divertor cassettes, two alternative are proposed and simulated by the CFD code ANSYS CFX [10]. The first design improvement is a coil in its original layout with additional cooling tube wrapped around its outer surface, and the second one is an actively water cooled coil.

5.3. Coil with a cooling tube

The overall dimensions of the coil and the boundary conditions are as stated in section 3 and 4, respectively. The inner diameter of the cooling tube is 3.5mm and the outer is 4mm. Due to the lack of symmetry in the helical cooling tube a half of the coil is modelled and meshed with the ANSYS program. A picture of the model could be seen in Fig.12. All parts of the coil arranged in a group of "components of nodes" or "components of elements" have been imported in ANSYS CFX. Different fluid and solid domains are created and their corresponding fluid-solid interfaces. The most robust combination of boundary conditions which are commonly used in ANSYS CFX is set in this case: at the inlet is applied a mass flow rate of 0.096 kg/s and a static temperature of 393.15K, and at the outlet a static pressure of 1.65MPa is applied. The time step for the fluid domain is set to be equal to length of the tube divided by the flow velocity, and the solid timescale is equal to 1000 sec.

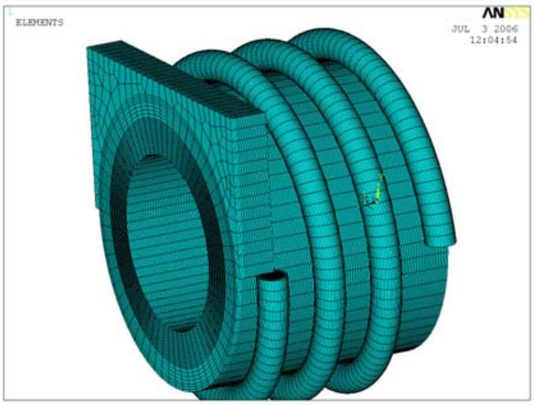

Figure 12: Coil with a cooling tube

The temperature distribution in half and quarter of the coil is shown in Fig.13 and Fig.14, respectively. The temperature difference is: 15.05°C in the coil, 13.6°C in the wire and 14°C in the former. It is observed that the temperature increase in the water next to the tube wall is just 1.6°C and the pressure drop at the outlet is 0.1183 Pa.

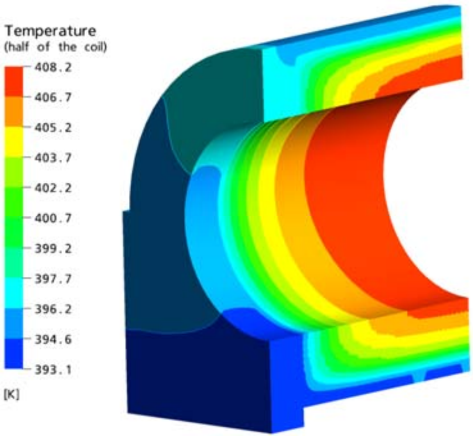

Figure 13: Temperature distribution in ¼ of the coil

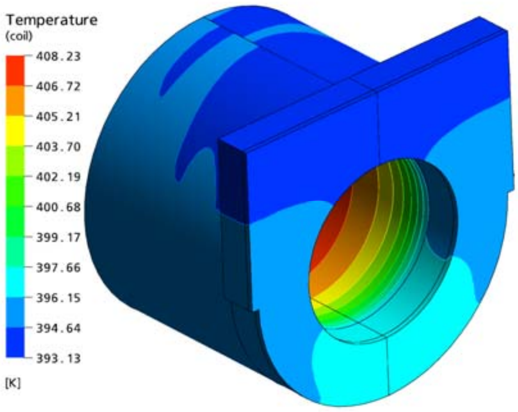

Figure 14: Temperature distribution in ½ of the coil

<u>5.4. Actively water cooled coil</u>

In this case, the coil will be immersed in a tube, made of stainless steel, through which flows water with a constant flow rate in a forced convection regime. The main advantage in this design, apart from the fact that the water foreseen for cooling the HHF divertor components could be used in this approach as well, will be cooling of the coil along its inner and outer surface and its two end plates. The support structures are also cooled and are therefore neglected. The new divertor coil consists of following elements, listed in sequential order: former, made of 0.5mm thick stainless steel, ceramic filler with thickness of 1.1 mm, conductor- ceramic coated steel wire, 4 layers x 0.7mm, 1.1 mm thick ceramic filler and stainless steel case with thickness of 0.5 mm. The dimensions of the coil are as follows: coil effective area is 2 m^2, the overall diameter of the coil is 80 mm and the inner diameter is 68mm, total number of turns 520. The dimensions of the cooling tube are: 100mm inner diameter, 106mm outer diameter and length 200mm. The material properties used in the CFX program are the same as the one listed in Table 1. For the thermal conductivity of ceramic a more optimistic value is considered now, 5 W/mK. With the aim of obtaining a much more better heat transfer between the fluid and the solid structure, a thick hexahedron mesh layer is modelled all around the surface of the coil and in the boundary layer next to the inner surface of the cooling tube. Fine meshing has been performed in the regions close to the walls in order to accurately calculate the viscous sublayer. At the inlet a static temperature of 393.15K and mass flow rate of 0.4 kg/s are applied and at the outlet a static pressure of 3.9MPa is set. Standard no-slip wall boundary conditions are adjusted. The most important parameter was the convergence criterion at each time step. It was found that the default CFX criterion of $1x10^{-4}$ under-predicts the magnitude of the velocities. The results achieved by convergence criteria of $1x10^{-5}$ are in a very good agreement with the analytical calculations. Due to the complex ANSYS meshing and the large number of elements only $1/4^{th}$ of the coil and tube was modeled. Symmetry boundary conditions over XY plane are applied, i.e. half of the coil is considered. Fig.15 and Fig.16 show the temperature distribution in ¼ of the coil using the SST turbulence model and the k-ε model, respectively. The water region is presented only as wireframe graphics and the tube is presented as solid structure.

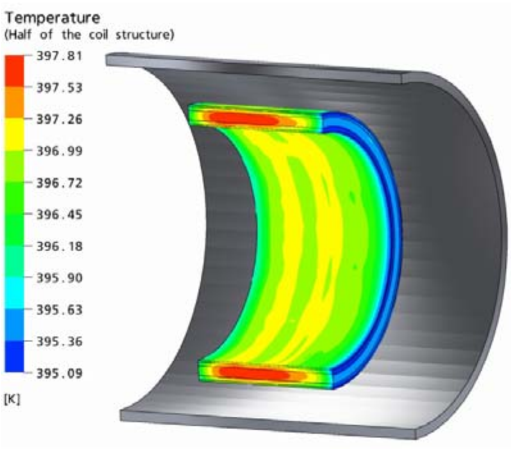

Figure 15: SST turbulence model

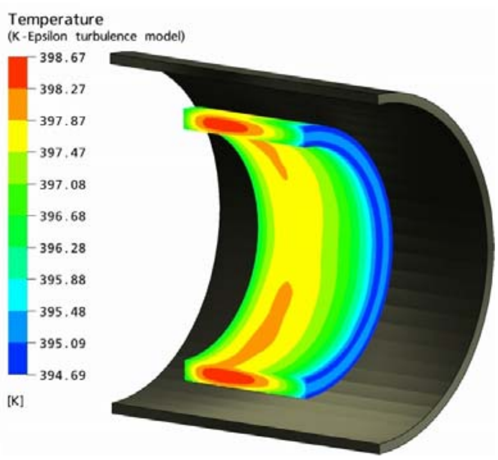

Figure 16: K-epsilon turbulence model

In our case the model is simulated according to two turbulence models and the fluid-structure interaction is observed:

1) The k-ε model is based on the eddy viscosity concept. It assumes that the turbulent viscosity is linked to the turbulence kinetic energy and dissipation via the expression:

$$\mu_t = C_\mu \rho \frac{k^2}{\varepsilon} \qquad \textbf{(Eq. 2)}$$

where C_μ is a constant, and μ_t is the turbulence viscosity [11].

2) The Shear Stress Transport (SST) k-ω based model. One advantage of this model is the near wall treatment for low-Reynolds number computations. It is more accurate and more robust than the k-ε model. The k-ω model assumes that the turbulence viscosity is linked to the turbulent kinetic energy and angular velocity via the relation:

$$\mu_t = \rho \frac{k}{\omega} \qquad \textbf{(Eq. 3)}$$

where k is the turbulent kinetic energy, and ω is the angular velocity (assumed that ω=f*2pi, where **f** is the frequency) .

The main problem with the Wilcox k-ω model [12] is its well known strong sensitivity to freestream conditions. Depending on the value specified for ω at the inlet, a significant variation in the results can be obtained. On the other hand, the near wall resolution of $y^+ < 0.2$ which is necessary requirements by the k-ε model, cannot be guaranteed in most applications. In order to solve the problem, a blending between the k-ω model near the surface and the k-ε model in the outer region was developed and introduced in the SST model. The k-ω model is thereby multiplied by a blending function F_1 and the transformed k-ε model by a function 1- F_1. F_1 is equal to one near the surface and switches over to zero inside the boundary layer (i.e. a function of the wall distance).

6: Conclusion

A series of investigations over variations of the ITER divertor coil design supported by ANSYS and CFX simulations were done in the present work. The aim was to keep the temperature variation in the winding pack within 10 K in order to reduce thermoelectric voltages to an acceptable level. Optimisation and reshaping of the coil, based only on cooling by conduction was not sufficient to meet this target. Therefore, an actively water cooled coil was designed and simulated by ANSYS CFX. According to the latest simulation, the temperature variation within the coil is about 2.8 K using the SST turbulence model and approximately 4K using the k-ε turbulence model. Even if we assume the more pessimistic result by applying the k-ε turbulence model, the actively cooled coil seems to be a reasonable solution matching both the new divertor design and divertor cooling conditions.

7: Acknowledgement

This report was prepared as an account of work undertaken within the framework of ITER Transitional Activities (ITA). These are conducted by the Participants: the European Atomic Energy Community, Japan, the People's Republic of China, the Republic of Korea, the Russian Federation, and the United States of America, under the auspices of the International Atomic Energy Agency. The views and opinions expressed herein do not necessarily reflect those of the Participants to the ITA, the IAEA or any agency thereof. Dissemination of the information in this paper is governed by the applicable terms of the former ITER EDA Agreement.

REFERENCES

[1] VAYAKIS, G et al. – Magnetic Diagnostics for ITER/BPX plasmas. Rev.Sci.Instrum, Vol.74, No. 4, Apr.2003

[2] VAYAKIS, G et al. - Radiation-induced Thermoelectric Sensitivity (RITES) in ITER prototype magnetic sensors. Rev.Sci.Instrum, Vol.75, Issue 10, pp.4324-4327, 2004

[3] VILA, R. and HODSON, E.R., J.Nucl.Mater., In press, 2006

[4] CHITARIN, G., GRANDO, L., PERUZZO, S., TACCONET, C. – Design developments for the ITER in-vessel equilibrium Halo current sensors. 24th SOFT Conference, Warsaw, Poland, Sept.2006, to be published in Fusion Engineering and Design

[5] HAANGE,R - Overview of remote maintenance scenarios for the ITER machine. Fusion Engineering and Design, Vol.27, pp.69-82, 1995

[6] ITER Final Design Report

[7] http://www.iter.org/pdfs/PDD2-4.pdf

[8] ANSYS, Engineering Analysis System, Release 10.0A1, ANSYS Inc.

[9] Brevier Technische Keramik, http://www.keramverband.de/brevier_dt/10/9/2/10_9_2.htm

[10] ANSYS CFX, Computational Fluid Dynamics, Release 10.0, ANSYS Inc.

[11] LAUNDER, B.E, REECE, G.J., RODI, W. – Progress in the development of a Reynolds stress turbulence model. Journal of Fluid Mechanics, Vol.68, No.3, pp.537-566, 1975

[12] WILCOX, D.C. - Multiscale model for turbulent flows. AIAA 24th Aerospace Sciences Meeting, American Institute of Aeronautics and Astronautics, 1986